

# MIMO Over-the-Air Computation for High-Mobility Multi-Modal Sensing

Guangxu Zhu and Kaibin Huang

**Abstract**—In future *Internet-of-Things* (IoT) networks, sensors or even access points can be mounted on ground/aerial vehicles for smart-city surveillance or environment monitoring. For such *high-mobility sensing*, it is impractical to collect data from a large population of sensors using any traditional orthogonal multi-access scheme as it would lead to excessive latency. To tackle the challenge, a technique called *over-the-air computation* (AirComp) was recently developed to enable a data-fusion to receive a desired function (e.g., averaging or geometric mean) of sensing data from concurrent sensor transmissions. This is made possible by exploiting the superposition property of a multi-access channel. Targeting a multi-antenna sensor network, this work aims at developing *multiple-input-multiple output* (MIMO) AirComp for enabling *high-mobility multi-modal sensing* where a multi-modal sensor monitors multiple environmental parameters such as temperature, pollution and humidity. To be specific, we design MIMO-AirComp equalization and channel feedback techniques for spatially multiplexing multi-function computation, each corresponding to a particular sensing-data type. Given the objective of minimizing sum mean-squared error via spatial diversity, a close-to-optimal equalizer is derived in closed-form using differential geometry. The solution can be computed as the weighted centroid of points (subspaces) on a Grassmann manifold, where each point represents the subspace spanned by the channel coefficient matrix of a sensor. As a by-product, the problem of MIMO-AirComp equalization is proved to have the same form as the classic problem of multicast beamforming, establishing the *AirComp-multicasting duality*. Its significance lies in making the said Grassmannian-centroid solution method transferable to the latter problem which otherwise is solved using the more computation-intensive *semidefinite relaxation* method in the literature. Last, building on the AirComp equalization solution, an efficient channel-feedback technique is designed for an access point to receive the equalizer from simultaneous sensor transmissions of designed signals that are functions of local channel-state information. This overcomes the difficulty of provisioning orthogonal feedback channels for many sensors.

## I. INTRODUCTION

Attaining the vision of *Internet-of-Things* (IoT) will require the ubiquitous deployment of an enormous number of sensors (e.g., tens of billions) in our society [1], [2]. The brute-force approach of “transmit-then-compute” is obviously impractical for this large-scale sensor network as the massive radio access would result in excessive network latency and low efficiency in spectrum utilization. The situation is exacerbated at high mobility where ultra-fast data aggregation from many sensors is desired. This is the case when sensors and/or the *access-point* (AP) are mounted on ground vehicles or *unmanned aerial vehicles* (UAV) for ubiquitous city surveillance in the smart-city application [see Fig. 1(a)], or for wild-area monitoring to

avoid natural disasters [see Fig. 1(b)]. Motivated by the need of ultra-fast data aggregation, an intelligent solution, known as *over-the-air computation* (AirComp), is proposed recently that exploits the signal-superposition property of a *multi-access channel* (MAC) to compute a class of so called *nomographic* functions of distributed sensing data via concurrent sensor transmissions (see Fig. 1), thereby integrating computation and communication [3], [4]. Examples of such functions are show in Table I. Unlike rate-centric wireless systems where simultaneous transmissions result in interference, the computation accuracy for a sensor network with AirComp may grow with the number of simultaneous sensors due to the sensing-noise averaging. In this paper, we aim to advance the area of AirComp by developing *multiple-input-multiple output* (MIMO) AirComp for next-generation multi-antenna multi-modal sensor networks. The technology supports *high-mobility multi-modal* (HMM) sensing by enabling multi-function computation via spatial multiplexing and accurate reception of the results by exploiting spatial diversity.

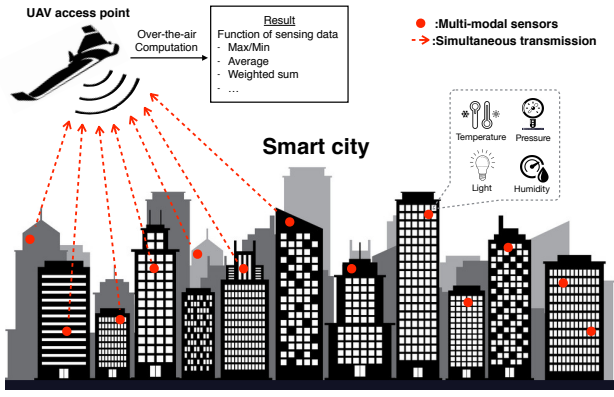
### A. Over-the-Air Computation for Sensor Networks

The idea of AirComp can be tracked back to the pioneer work studying functional computation in sensor networks [4].<sup>1</sup> In [4], structured codes (e.g., lattice codes) are designed for reliably computing at an AP a function of distributed sensing values transmitted over a MAC. The significance of the work lies in its counter-intuitive finding that “interference” can be harnessed to help computing. Subsequently, it was proved that the simple analog transmission without coding, where transmitted signals are scaled versions of sensing values, can achieve the minimum functional distortion achievable by any scheme [6]. On the other hand, coding can be still useful for other settings such as sensing correlated Gaussian sources [7]. The satisfactory performance (with optimality in certain cases) of simple *analog AirComp* have led to an active area focusing on designing and implementing techniques for receiving a desired function of concurrent signals, namely a targeted coherent combination of the signal waveforms [3], [8]–[16]. In particular, considering analog AirComp, power control at sensors was optimized in [8], [9], the computation rate (defined as the number of functional values computed per time slot) analyzed in [10], and the effect of channel estimation error characterized in [11].

The implementation of AirComp faces several practical issues. One is the synchronization of all active sensors required

G. Zhu and K. Huang are with the Dept. of EEE of The University of Hong Kong (HKU), Pok Fu Lam, Hong Kong. Corresponding author: K. Huang (Email: haungkb@eee.hku.hk).

<sup>1</sup>AirComp also appeared the same time as a key operation in the scheme named physical-layer network coding in [5].



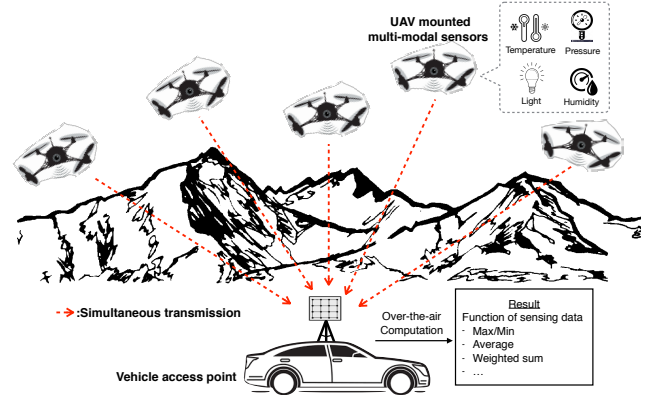
(a) Smart-city surveillance with UAV mounted access point

Figure 1. Two scenarios for high-mobility multi-modal sensing.

for coherent combining at the AP. To cope with synchronization errors, a scheme was proposed in [12], [13] where the sensing value is modulated at each sensor as the power of transmitted signal and furthermore a random phase rotation is applied to the signal. The design transforms functional computation at the receiver to power detection while synchronization error appears as random noise. An alternative solution, called *AirShare*, was developed in [14] for synchronizing sensors by broadcasting a reference-clock signal and its effectiveness was demonstrated using a prototype. In addition, by applying appropriate data pre/post-processing, later work extended and implemented AirComp to compute a variety of functions besides the linear ones (as summarized in Table I) [15], [16].

It is worth mentioning that the coding techniques designed for AirComp in computing-centric sensor networks [4] inspired researchers to adopt relevant principles and ideas in designing new schemes for rate-centric communication networks [17]–[21]. For relay assisted networks, the application of AirComp at relay nodes for decoding and forwarding linear functions of the transmitted messages led to the invention of the well known *compute-and-forward* relaying schemes [17]–[19]. Building on lattice coding, a novel so called integer-forcing linear receiver was proposed for spatial multiplexing in a *multiple-input-multiple-output* (MIMO) system that attempts to create an effective channel matrix with integer coefficients to facilitate lattice decoding. The key operation, integer forcing, is similar to AirComp and computes a desired set of linear functions with integer coefficients [20], [21]. In parallel with the above research, extensive progresses were made in the area of physical layer network coding where the celebrated network coding schemes invented for wired networks were extended to wireless networks with AirComp relays (see survey in [22]).

Sensing devices targeting emerging applications such as smart cities are sophisticated. Each typically contains multiple multi-modal sensors monitoring different environmental parameters (e.g., pressure, light, humidity, and temperature) [23]. In particular, a smartphone recruited for crowd-sensing typically contains seven or more sensors such as inertial, GPS, and light sensors [24]. In view of prior work, the existing solutions focus only single-function AirComp assuming single-antenna sensors having uni-modal sensing capabilities. However, next-generation wireless networks equipped with large-scale arrays



(b) Wild-area monitoring with UAV mounted sensors

will make it possible to simultaneously compute multiple functions of multi-modal sensing data over-the-air. This inspires the current work on developing the technology of AirComp for a MIMO MAC, which can simultaneously spatial multiplex multi-function computation and suppress computation errors by exploiting spatial-diversity gain. Thereby, the data-fusion latency in sensor networks can be substantially reduced, meeting the ultra-low latency requirement in next-generation networks especially when high-mobility support is needed [1].

### B. MIMO Beamforming: Multi-Access versus AirComp

Beamforming design for multiuser MIMO systems is a classic topic that has been extensively studied and there exists a rich relevant literature [25]–[27]. In terms of network topology, the multi-antenna multi-modal sensor network we consider is equivalent to a MIMO multi-access communication network where a single AP supports simultaneous uplink transmissions of multiple users. For the communication network, the designs of multiuser MIMO beamforming at the AP can be largely grouped into capacity-achieving nonlinear designs based on *successive interference cancellation* (SIC) [25] and low-complexity linear designs (*minimum mean-squared error* (MMSE) or zero-forcing) [26]–[28]. All of the designs share the same objective of decoupling multiuser signals by interference suppression and spatial multiplexing of data streams for each user. In contrast, AirComp receive beamforming in the sensor network has a different objective of minimizing the total distortion in the received values of multiple functions combining multi-modal data simultaneously sent by a set of sensors. Due to the difference in objective between communication and sensing, the known designs for the former are inapplicable for the latter. On the other hand, existing AirComp literature considers only uni-function computation targeting uni-modal sensing as discussed earlier. This makes receive beamforming for multi-function AirComp for multi-modal sensing an uncharted problem to be tackled in this work.

It is worth mentioning that the discovery of *uplink-downlink duality* is a breakthrough in multiuser MIMO communication. The duality reveals similar structures in optimal beamformers for the MACs and broadcast channels that exist under various performance criteria ranging from capacity maximization [29], [30] to MMSE [31]. This allows beamforming designs derived

Table I

EXAMPLES OF NOMOGRAPHIC FUNCTIONS (SEE DEFINITION 1) THAT ARE AIRCOMPUTABLE.

Name	Expression
Arithmetic Mean	$h = \frac{1}{K} \sum_{k=1}^K d_k$
Weighted Sum	$h = \sum_{k=1}^K \omega_k d_k$
Geometric Mean	$h = \left( \prod_{k=1}^K d_k \right)^{1/K}$
Polynomial	$h = \sum_{k=1}^K \omega_k d_k^{\beta_k}$
Euclidean Norm	$h = \sqrt{\sum_{k=1}^K d_k^2}$

for the MACs to be applied to the broadcast channels where the optimal beamforming design was largely an open problem prior to the finding of the duality. Inspired by this finding, we address a similar question in the current work: *What is the downlink dual of the (uplink) AirComp beamforming for sensor networks?*

### C. Contributions and Organization

We consider a multi-antenna multi-modal sensor network where a multi-antenna AP performing fusion of data transmitted by a cluster of multi-antenna multi-modal sensors. By measuring multiple time-varying parameters of the environment, each sensor generates multiple data streams. In each time slot, a sensor transmits a set of multi-modal data values in the analog way, namely by amplitude modulation [12], [13], over multiple antennas. The transmissions of all sensors are simultaneous. The AP attempts to jointly receive multiple *nomographic functions* (such as those in Table I) of distributed sensor data by AirComp and spatial multiplexing. The AirComp of a nomographic function is implemented by three cascaded operations: 1) pre-processing at sensors, 2) weighted summation of preprocessed outputs by simultaneous transmissions, and 3) post-processing at the AP [3], [12], [13]. In the current scenario, transmit and receive beamforming are applied to spatially multiplex multi-function AirComp as well as exploit spatial diversity to minimize the distortion of function values caused by noise, which is measured by sum *mean-squared error* (MSE) over functions.

While the traditional uni-function AirComp is a simple technique, the proposed multi-function version is challenging with the optimization of receive beamforming proved to be NP-hard. Specifically, for uni-function AirComp, channel inversion at each sensor yields a desired weighted sum of preprocessed data at the AP, giving the desired function value after post-processing [3]. For multi-function AirComp, channel inversion remains optimal as shown in this work and is implemented by zero-forcing beamforming. Nevertheless, receive beamforming for multi-function AirComp, referred to as *MIMO-AirComp equalization*, is a new design problem that finds no relevant result in the AirComp literature. The equalizer optimization is non-convex but can be relaxed as a *semidefinite programming* (SDP) problem and thus solved using an iterative interior point algorithm. The standard approach does not yield any insight into the optimal equalizer structure and more importantly does not lead to an efficient channel-feedback design for acquiring the equalizer at the AP. To address these issues, we impose an orthogonality constraint on the AirComp equalizer, which is a technique for approximate

beamformer design and limited channel feedback as widely applied in the literature [32]–[35]. Concretely, this allows a close-to-optimal equalizer to be derived in closed-form using tools from differential-geometry, revealing an interesting geometry structure in the design. Moreover, the closed-form solution leads to an efficient channel feedback design that exploits the AirComp architecture for direct equalizer acquisition at the AP from simultaneous feedback by all sensors.

The main contributions of this work are summarized as follows.

- **Multi-Function AirComp Beamforming:** As mentioned, while zero-forcing transmit beamforming is found to be optimal, the receive-beamformer optimization for sum-MSE minimization under transmission-power constraints can be proved to be NP-hard. By tightening the constraints, the resultant approximate problem is found to involve optimization on a Grassmann manifold, which can be interpreted as the space of subspaces. This allows the application of differential geometry to solve the approximate problem. The derived solution shows the normalized receive beamformer to be the *weighted centroid of a cluster of points on the manifold*, where each point represents the eigen-subspace of an individual MIMO channel and the corresponding weight its smallest eigenvalue. In addition, the optimal beamformer norm is also derived in closed-form. Such a beamformer design allowing efficient computation is verified by simulation to be close-to-optimal.
- **AirComp-Multicasting Duality:** As a by-product of our investigation, for the special case of AirComp with single-antenna (uni-modal) sensors, the problem of receive-beamforming optimization is discovered to have the identical form as the classic problem of multicast transmit-beamforming, thereby establishing a novel *AirComp-multicasting duality*. The latter problem is known to be NP-hard and typically solved using the *semidefinite relaxation* (SDR) method. The significance of our finding lies in allowing the solution method for AirComp beamforming to be transferable to multicast-beamforming. This yields a new solution method for the latter with complexity much lower than the existing SDR approach as the network scales up.
- **AirComp Channel Feedback:** Last, we solve the *AirComp feedback* problem: How to efficiently acquire the derived AirComp beamformer at the AP, which depends on global *channel-state information* (CSI), by sensor distributed transmissions based on *local CSI*? Given channel reciprocity, it is discovered that the AirComp system architecture can be also used for efficient feedback. The resultant number of feedback rounds is *independent* of the sensor population, overcoming the drawback of traditional channel training. Novel feedback techniques are designed for sequential feedback of the normalized AirComp beamformer and beamformer norm based on their derived expressions, where each feedback round involves concurrent transmissions by all sensors. Essentially, the two techniques implement AirComp of two functions, namely the weighted centroid of a set of matrices and

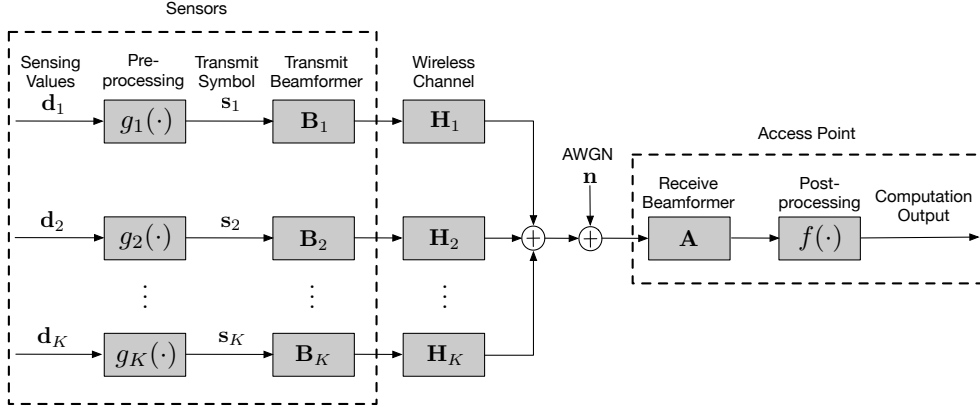


Figure 2. System model of AirComp via MIMO transmission.

the maximum of a set of scalar values. They are hence exclusively for multi-function AirComp and may not be applicable for traditional multiuser MIMO communication systems where multiuser feedback requires orthogonal channels and focuses on precoder quantization [36], [37].

The remainder of the paper is organized as follows. Section II introduces the AirComp system model. Section III presents the problem formulation for the enabling beamforming design and channel feedback. The proposed beamforming design is presented in Section IV, and the duality between the uplink AirComp and downlink multicasting is discussed in Section V. Section VI proposes an efficient channel-feedback scheme that can be implemented by AirComp. Simulation results are provided in Section VII, followed by concluding remarks in Section VIII.

## II. SYSTEM MODEL

We consider a wireless sensor network consisting of  $K$  multi-modal sensors and a single AP as illustrated in Fig.2. All nodes are equipped with antenna arrays. Specifically,  $N_t$  antennas are deployed at each sensor and  $N_r$  at the AP. Each multi-modal sensor records the values of  $L$  heterogeneous time-varying parameters of the environment, e.g., temperature, pollution, and humidity. The data from the record of the  $\ell$ -th parameter is referred to as type- $\ell$  data. For an arbitrary time slot, the measurement vector of the  $k$ -th sensor, grouping  $L$  sample values, is denoted by  $\mathbf{d}_k = [d_{k1}, d_{k2}, \dots, d_{kL}]^T \in \mathbb{R}^{L \times 1}$ , where  $d_{k\ell}$  is the measurement of the parameter  $\ell$  at sensor  $k$ . Instead of collecting the whole data set, the AP aims at computing  $L$  functions of  $L$  corresponding types of data, denoted by  $\{h_\ell(d_{1\ell}, \dots, d_{K\ell})\}_{\ell=1}^L$ , to support ultra-fast HMM sensing. The class of functions that are computable by AirComp are called *nomographic functions* as defined below.

**Definition 1** (Nomographic Function [13]). The function  $h_\ell(d_{1\ell}, \dots, d_{K\ell})$  is said to be nomographic, if there exist  $K$  preprocessing functions  $g_{k\ell}(\cdot) : \mathbb{R} \rightarrow \mathbb{R}$  along with a post-processing function  $f_\ell(\cdot) : \mathbb{R} \rightarrow \mathbb{R}$  such that it can be represented in the form:

$$h_\ell(d_{1\ell}, \dots, d_{K\ell}) = f_\ell \left( \sum_{k=1}^K g_{k\ell}(d_{k\ell}) \right). \quad (1)$$

Some common nomographic functions are listed in Table I. Based on the nested form of (1), the AirComp of a

nomographic function can be implemented in the sensor network by three operations as illustrated in Fig. 2: 1) pre-processing at each sensor specified by  $g_k = \{g_{k\ell}(\cdot)\}$  where  $g_{k\ell}$  operates on the type- $\ell$  data at sensor  $k$ , 2) summation of preprocessed data realized by multi-access, and 3) post-processing at the AP. Considering the computation of the geometric mean of type- $\ell$  data as an example, the pre-processing  $g_{k\ell}(x) = \log x$ , and the post-processing  $f_\ell(y) = \exp(y/K)$ . Let  $\mathbf{s}_k = [g_{k1}(d_{k1}), g_{k2}(d_{k2}), \dots, g_{kL}(d_{kL})]^T$  denote the multi-modal symbol vector after preprocessing and  $\mathbf{h} = [h_1, h_2, \dots, h_L]^T$  the AirComputed function values. For ease of transmission-power control and without loss of generality, the symbols are assumed to be normalized to have unit variance, i.e.,  $\mathbb{E}\{\mathbf{s}_k \mathbf{s}_k^H\} = \mathbf{I}$ , where the normalization factor for each data type is uniform for all sensors and can be inverted at the AP. Given the one-to-one mapping between  $\mathbf{s} = \sum_{k=1}^K \mathbf{s}_k$  and  $\mathbf{h}$  according to (1), we refer to  $\mathbf{s}$  as the *target-function vector* for ease of exposition.

### A. AirComp Phase

Assuming symbol-level synchronization<sup>2</sup>, all users transmit their symbol vectors simultaneously using their arrays. The distortion of the received vector with respect to the target-function vector due to MIMO channels and noise is suppressed using transmit and receive beamforming. In other words, the joint beamforming attempts to attain coherent combining of  $K$  symbol vectors at the AP. Let  $\mathbf{A} \in \mathbb{C}^{N_r \times L}$  denote the receive beamforming matrix and  $\mathbf{B}_k \in \mathbb{C}^{N_t \times L}$  the transmit beamforming matrix at sensor  $k$ . Then the symbol vector received by the AP after receive beamforming is given as

$$\hat{\mathbf{s}} = \mathbf{A}^H \sum_{k=1}^K \mathbf{H}_k \mathbf{B}_k \mathbf{s}_k + \mathbf{A}^H \mathbf{n}, \quad (2)$$

where  $\mathbf{H}_k \in \mathbb{C}^{N_r \times N_t}$  represents the MIMO channel matrix for the link from the sensor  $k$  to the AP, and  $\mathbf{n}$  is the *additive white Gaussian noise* (AWGN) vector with *independent and identically distributed* (i.i.d.)  $\mathcal{CN}(0, \sigma_n^2)$  elements. The distortion of  $\hat{\mathbf{s}}$  with respect to  $\mathbf{s}$ , which quantifies the AirComp performance, is measured by the MSE defined as follows:

$$\text{MSE}(\hat{\mathbf{s}}, \mathbf{s}) = \mathbb{E} [\text{tr}((\hat{\mathbf{s}} - \mathbf{s})(\hat{\mathbf{s}} - \mathbf{s})^H)]. \quad (3)$$

<sup>2</sup>This can be achieved by broadcasting a common reference clock from the AP to sensors using the AirShare solution developed in [14].

Substituting (2) into (3), the MSE can be explicitly written as a function of the transmit and receive beamformer as follows:

$$\text{MSE}(\mathbf{A}, \{\mathbf{B}_k\}) = \sum_{k=1}^K \text{tr}((\mathbf{A}^H \mathbf{H}_k \mathbf{B}_k - \mathbf{I})(\mathbf{A}^H \mathbf{H}_k \mathbf{B}_k - \mathbf{I})^H) + \sigma_n^2 \text{tr}(\mathbf{A}^H \mathbf{A}). \quad (4)$$

The beamformers are optimized in the sequel under the criteria of MMSE.

### B. Channel Feedback Phase

Consider the existence of channel reciprocity and assume that perfect local CSI is available at all sensors. One can infer from (4) that computing the MMSE receive beamformer requires global CSI, namely  $\{\mathbf{H}_k\}$ . As mentioned, the naive approach of estimating the global CSI would incur long latency and large overhead when the number of sensors is large, thus is impractical for the ultra-fast HMM sensing applications. An intelligent channel-feedback design is proposed in the sequel to allow beamformer acquisition via concurrent transmissions by all sensors. Let  $\mathbf{X}_k \in \mathbb{C}^{N_t \times T}$  denote the signal matrix transmitted by sensor  $k$  where  $T$  is the signal length in symbol. Given typical high transmission power for channel training and feedback, the feedback observation at the AP can be assumed to be noiseless and thus be represented by an  $N_r \times T$  matrix  $\mathbf{Y}$  as follows:

$$\text{(AirComp Feedback)} \quad \mathbf{Y} = \sum_{k=1}^K \mathbf{H}_k \mathbf{X}_k. \quad (5)$$

As is clear in the sequel, with proper design of  $\{\mathbf{X}_k\}$ ,  $\mathbf{Y}$  can serve as a sufficient surrogate of the global CSI  $\{\mathbf{H}_k\}$  in beamformer computation at the AP.

## III. PROBLEM FORMULATION

### A. AirComp Beamforming Problem

Consider the joint optimization of the transmit and receive beamformers under the MMSE criterion and the transmission-power constraints. It is assumed that the average transmission power of each sensor cannot exceed a given positive value  $P_0$ . Since the transmitted symbols have unit variance, the power constraints are given as

$$\|\mathbf{B}_k\|^2 \leq P_0, \quad k = 1, 2, \dots, K. \quad (6)$$

Following a common approach in the MIMO beamforming literature (see e.g., [32]–[35]), the receive beamformer  $\mathbf{A}$  is constrained to be orthonormal matrix. As mentioned, the constraint can lead to a closed-form suboptimal solution with only marginal performance loss and furthermore facilitate efficient channel feedback design as presented in Section VI. As pointed out in [35], for most communication objectives, it is the subspace spanned by the beamformer but not the exact beamformer that has a crucial effect on the system performance, justifying the said constraint. Furthermore, under the MMSE criterion, a positive scaling factor  $\eta$ , called *denoising factor*, is included in  $\mathbf{A}$  for regulating the tradeoff between noise reduction and transmission-power control. To be specific, reducing  $\eta$  suppresses noise but requires larger transmission

power to maintain the MSE of computed function values. Mathematically, we can write  $\mathbf{A} = \sqrt{\eta} \mathbf{F}$  with  $\mathbf{F}$  being a tall unitary matrix and thus  $\mathbf{F}^H \mathbf{F} = \mathbf{I}$ . Then given the MSE in (4), the MMSE beamforming problem can be formulated as:

$$\begin{aligned} \text{(P1)} \quad & \min_{\eta, \mathbf{A}, \{\mathbf{B}_k\}} \text{MSE}(\mathbf{A}, \{\mathbf{B}_k\}) \\ & \text{s.t. } \|\mathbf{B}_k\|^2 \leq P_0, \quad \forall k, \\ & \mathbf{A}^H \mathbf{A} = \eta \mathbf{I}. \end{aligned}$$

The problem is solved in Section IV.

### B. AirComp Channel Feedback Problem

We propose the use of the AirComp architecture in Fig. 2 to realize the mentioned receive-beamformer acquisition by concurrent transmissions by all sensors. Let  $\mathbf{A}^*$  denote the derived beamformer solution to problem P1 and  $\tilde{f}$  and  $\tilde{g}_k$  be the feedback counterparts of the AirComp operations  $f$  and  $g_k$  (see Fig. 2). The key design constraint is that the transmitted signal  $\mathbf{X}_k$  in (5) must be a function of local CSI  $\mathbf{H}_k$  only, denoted as  $\mathbf{X}_k = \tilde{g}_k(\mathbf{H}_k)$ . Then it follows that

$$\text{(P2)} \quad \mathbf{A}^* = \tilde{f} \left( \sum_{k=1}^K \mathbf{H}_k \tilde{g}_k(\mathbf{H}_k) \right).$$

and the problem of AirComp feedback design reduces to the design of the functions  $\tilde{f}$  and  $\{\tilde{g}_k\}$ . The solution is presented in Section VI.

## IV. MULTI-FUNCTION AIRCOMP: BEAMFORMING

In this section, the AirComp beamforming problem in Problem P1 is solved. While zero-forcing transmit beamforming can be proved to be optimal, the receive beamforming optimization is found to be NP-hard. An approximate problem is obtained by tightening the power constraints. This problem allows a practical solution approach based on *differential geometry*. The solution reveals that the optimal receive beamformer can be approximated by the weighted centroids of a cluster of points on a Grassmann manifold, each corresponding to the subspace of an individual MIMO channel. To facilitate exposition, some basic definitions and principles of Grassmann manifolds are provided in Appendix A.

Problem P1 is difficult to solve due to its non-convexity. The lack of convexity arises from the coupling between transmit and receive beamformers in the objective function, and the orthogonality constraint on the receive beamformer. To simplify the problem, zero-forcing transmit beamforming conditioned on a receive beamformer is first shown to be optimal as follows.

**Lemma 1.** Given a receive beamformer  $\mathbf{A}$ , the MSE objective stated in (4) is minimized by the following zero-forcing transmit beamformers:

$$\mathbf{B}_k^* = (\mathbf{A}^H \mathbf{H}_k)^H (\mathbf{A}^H \mathbf{H}_k \mathbf{H}_k^H \mathbf{A})^{-1}, \quad \forall k. \quad (7)$$

*Proof:* See Appendix B. ■

We note that the power constraint imposed on the precoder  $\mathbf{B}_k$  will be enforced in the sequel via regulating the norm of the equalizer  $\mathbf{A}$ , or equivalently, the denoising factor  $\eta$ .

**Remark 1** (Number of AirComputable Functions). Note that to ensure matrix  $\mathbf{A}^H \mathbf{H}_k \mathbf{H}_k^H \mathbf{A}$  is invertible, it requires  $L \leq \min\{N_t, N_r\}$ . This implies that, the number of functions that can be simultaneously computed by the proposed multi-function AirComp is limited by  $\min\{N_t, N_r\}$ . The result is due to the underpinning limit of MIMO spatial multiplexing: the maximum number of spatial streams is  $\min\{N_t, N_r\}$ .

By substituting (7) in Lemma 1, Problem P1 is transformed to the equivalent problem of minimizing the denoising factor of the receive beamformer:

$$\begin{aligned}
 (\text{P3}) \quad & \min_{\eta, \mathbf{F}} \eta \\
 & \text{s.t. } \frac{1}{\eta} \text{tr}((\mathbf{F}^H \mathbf{H}_k \mathbf{H}_k^H \mathbf{F})^{-1}) \leq P_0, \forall k, \\
 & \mathbf{F}^H \mathbf{F} = \mathbf{I},
 \end{aligned}$$

where  $\mathbf{F}$  is defined earlier as the normalized receive beamformer. Though Problem P3 has a simpler form than P1, it remains non-convex due to the non-convex orthonormal constraint of the receive beamformer. In fact, Problem P3 is found in the next section to be NP-hard via proving its equivalence to the NP-hard multicast beamforming problem. To develop a tractable approximation of the problem, a reasonable modification of the power constraints is derived. To this end, a useful inequality is obtained as shown below.

**Lemma 2.** Let  $\mathbf{H}_k = \mathbf{U}_k \Sigma_k \mathbf{V}_k^H$  denote the compact form of *singular value decomposition* (SVD) of  $\mathbf{H}_k$ . Then we have the following inequality:

$$\text{tr}((\mathbf{F}^H \mathbf{H}_k \mathbf{H}_k^H \mathbf{F})^{-1}) \leq \frac{L}{\lambda_{\min}(\Sigma_k^2) \lambda_{\min}(\mathbf{U}_k^H \mathbf{F} \mathbf{F}^H \mathbf{U}_k)}, \quad (8)$$

where the equality holds given a well-conditioned channel, i.e.,  $\Sigma_k = \lambda \mathbf{I}$  for some constant  $\lambda$ .

*Proof:* See Appendix C. ■

Tightening the power constraints in Problem P3 using Lemma 2 gives the approximate problem:

$$\begin{aligned}
 (\text{P4}) \quad & \min_{\eta, \mathbf{F}} \eta \\
 & \text{s.t. } \eta \lambda_{\min}(\mathbf{U}_k^H \mathbf{F} \mathbf{F}^H \mathbf{U}_k) \geq \frac{L}{P_0 \lambda_{\min}(\Sigma_k^2)}, \forall k, \\
 & \mathbf{F}^H \mathbf{F} = \mathbf{I}.
 \end{aligned}$$

Since the feasible set of Problem P4 is smaller than that of P3, the solution to P4 is a feasible solution though potentially a suboptimal one to P3. To solve Problem P4 using differential geometry, an equivalent form containing subspace distances between the receive beamformer and individual MIMO channels is obtained as follows.

**Lemma 3.** The problem P4 and the following problem P5 are equivalent.

$$\begin{aligned}
 (\text{P5}) \quad & \min_{\mathbf{F}} \max_k \lambda_{\min}(\Sigma_k^2) (d_{P2}^2(\mathbf{U}_k, \mathbf{F}) - 1) \\
 & \text{s.t. } \mathbf{F}^H \mathbf{F} = \mathbf{I},
 \end{aligned}$$

where  $d_{P2}^2(\mathbf{U}_k, \mathbf{F})$  denotes the projection 2-norm distance between the subspaces spanned by  $\mathbf{U}_k$  and  $\mathbf{F}$  [see (25) in Appendix A].

*Proof:* See Appendix D. ■

Problem P5 is not yet in a ready form admitting the differential-geometry solution approach and requires an additional approximation. For this purpose, the objective function is bounded below.

**Lemma 4.** The objective function in Problem P5 can be bounded as follows:

$$\begin{aligned}
 & \frac{1}{K} \sum_{k=1}^K \lambda_{\min}(\Sigma_k^2) d_{P2}^2(\mathbf{U}_k, \mathbf{F}) - \frac{c}{K} \\
 & \leq \max_k \lambda_{\min}(\Sigma_k^2) (d_{P2}^2(\mathbf{U}_k, \mathbf{F}) - 1) \\
 & \leq \sum_{k=1}^K \lambda_{\min}(\Sigma_k^2) d_{P2}^2(\mathbf{U}_k, \mathbf{F}) - c, \quad (9)
 \end{aligned}$$

where we define  $c = \sum_{k=1}^K \lambda_{\min}(\Sigma_k^2)$  which is a constant independent of the control variable  $\mathbf{F}$ .

The proof is straightforward and omitted for brevity. Approximating the objective function in P5 by either the lower or the upper bound in Lemma 4 both lead to the same approximate problem which is given by:

$$\begin{aligned}
 (\text{P6}) \quad & \min_{\mathbf{F}} \sum_{k=1}^K \lambda_{\min}(\Sigma_k^2) d_{P2}^2(\mathbf{U}_k, \mathbf{F}) \\
 & \text{s.t. } \mathbf{F}^H \mathbf{F} = \mathbf{I}.
 \end{aligned}$$

**Remark 2** (Beamformer Geometric Interpretation). Problem P6 allows a geometric interpretation of the desired receive beamformer  $\mathbf{F}^*$ . In fact, the problem is to find a *weighted centroid* of a set of points (each being a subspace)  $\{\mathbf{U}_k\}$  on a Grassmann manifold with the squared projection 2-norm as the distance metric, where the weights are  $\{\lambda_{\min}(\Sigma_k^2)\}$ . This reveals that the receive beamformer makes the best-effort to be aligned with all the  $K$  MIMO channel matrices with the alignment (subspace) distances adjusted by corresponding channel gains as specified by the smallest channel eigenvalues.

Problem P6 can be approximately solved by a closed-form solution that can be efficiently computed without resorting to an iterative algorithm. Particularly, the closed-form solution can be derived by replacing the projection 2-norm distance  $d_{P2}$  with the projection F-norm  $d_{PF}(\mathbf{U}_k, \mathbf{F})$  (see Appendix A). Note that  $d_{P2}(\mathbf{U}_k, \mathbf{F}) \approx d_{PF}(\mathbf{U}_k, \mathbf{F})$  for a small principal angle [38] and are exactly equivalent in the case of  $N_t = 1$  according to (27). Thus, the problem P6 can be approximated as

$$\begin{aligned}
 & \min_{\mathbf{F}} \sum_{k=1}^K \lambda_{\min}(\Sigma_k^2) d_{PF}^2(\mathbf{U}_k, \mathbf{F}) \\
 & \text{s.t. } \mathbf{F}^H \mathbf{F} = \mathbf{I}, \quad (10)
 \end{aligned}$$

which still seeks a weighted centroid of channel subspaces as before but based on a different subspace distance metric. According to the definition in (26),  $d_{PF}^2(\mathbf{U}_k, \mathbf{F})$  can be computed in a matrix form by

$$d_{PF}^2(\mathbf{U}_k, \mathbf{F}) = N_t - \text{tr}(\mathbf{U}_k^H \mathbf{F} \mathbf{F}^H \mathbf{U}_k).$$

Then, substituting it to the objective function in Problem P7, the problem can be equivalently written as

$$\begin{aligned}
 (\text{P7}) \quad & \max_{\mathbf{F}} \sum_{k=1}^K \lambda_{\min}(\Sigma_k^2) \text{tr}(\mathbf{U}_k^H \mathbf{F} \mathbf{F}^H \mathbf{U}_k) \\
 & \text{s.t. } \mathbf{F}^H \mathbf{F} = \mathbf{I}. \quad (11)
 \end{aligned}$$

Problem P7 remains non-convex due to 1) maximizing a convex objective function and 2) the orthogonality constraints on the variable  $\mathbf{F}$ . Nevertheless, by intelligently constructing an equivalent unconstrained problem, we are able to derive a closed-form solution for Problem P7 (see the following Lemma 5) via analyzing the stationary points of the unconstrained problem. For ease of exposition, define a matrix  $\mathbf{G} \in \mathbb{C}^{N_r \times N_r}$ , called *effective CSI*, as follows:

$$\text{(Effective CSI)} \quad \mathbf{G} = \sum_{k=1}^K \lambda_{\min}(\Sigma_k^2) \mathbf{U}_k \mathbf{U}_k^H. \quad (12)$$

As shown shortly in Lemma 5, the normalized AirComp receive beamformer  $\mathbf{F}^*$  depends on the global CSI via the effective CSI. In other words,  $\mathbf{G}$  is sufficient for computing  $\mathbf{F}^*$ .

**Lemma 5.** Let  $\mathbf{G} = \mathbf{V}_G \Sigma_G \mathbf{V}_G^H$  be the SVD of  $\mathbf{G}$  given in (12). The solution of Problem P7 is given by the first  $L$  principal eigen-vectors of  $\mathbf{G}$ , namely

$$\mathbf{F}^* = [\mathbf{V}_G]_{:,1:L}. \quad (13)$$

*Proof:* See Appendix E. ■

Finally, combining Lemmas 1 - 5, the proposed MMSE beamforming design for multi-function AirComp is summarized as follows:

- Receive Beamformer :  
 $\mathbf{A}^* = \sqrt{\eta^*} \mathbf{F}^*$ , with  $\mathbf{F}^*$  in (13),
- Denoising Factor :  
 $\eta^* = \max_k \frac{1}{P_0} \text{tr}(((\mathbf{F}^*)^H \mathbf{H}_k \mathbf{H}_k^H \mathbf{F}^*)^{-1}),$
- Transmit Beamformer :  
 $\mathbf{B}_k^* = ((\mathbf{A}^*)^H \mathbf{H}_k)^H ((\mathbf{A}^*)^H \mathbf{H}_k \mathbf{H}_k^H \mathbf{A}^*)^{-1}, \quad \forall k,$

(14)

where the denoising factor  $\eta^*$  is derived by examining the power constraints in Problem P3.

## V. AIRCOMP-MULTICASTING DUALITY

In this section, consider the case of single-antenna unimodal sensors. The AirComp receive-beamforming problem for uplink sensing-data collection is shown to be equivalent to the well known problem of transmit beamforming for downlink multicasting (see Fig. 3). This establishes the AirComp-multicasting duality, allowing the low-complexity beamforming design in the preceding section to be transferable to solve the NP-hard multicast beamforming problem.

### A. Review of the Multicast Beamforming Problem

Consider the scenario that multiple single-antenna users request the same data stream from a multi-antenna AP equipped as shown in Fig. 3(a). Assuming global CSI is available at AP, the problem of multicast beamforming is to minimize the total transmission power subject to a set of *signal-to-noise-ratio* (SNR) constraints specifying the users' quality-of-service requirements. Mathematically, the problem can be formulated as follows:

$$\begin{aligned} & \min_{\mathbf{w}} \|\mathbf{w}\|^2 \\ & \text{s.t.} \quad \frac{\|\mathbf{h}_k^H \mathbf{w}\|^2}{\sigma_k^2} \geq \gamma_k, \quad k = 1, 2, \dots, K, \end{aligned} \quad (15)$$

where  $\mathbf{w}$  denotes the multicast beamforming vector,  $\mathbf{h}_k$ ,  $\sigma_k^2$  and  $\gamma_k$  are the channel vector, noise variance and target SNR of user  $k$ , respectively. The problem can be proved to be NP-hard [39]. Nevertheless, it is known that a close-to-optimal solution can be efficiently computed using the well known SDR technique. The key idea of SDR is to recast the problem as an equivalent rank-one constrained SDP by denoting  $\mathbf{W} = \mathbf{w}\mathbf{w}^H$  as follows:

$$\begin{aligned} & \min_{\mathbf{W}} \text{tr}(\mathbf{W}) \\ & \text{s.t.} \quad \frac{1}{\gamma_k \sigma_k^2} \text{tr}(\mathbf{h}_k \mathbf{h}_k^H \mathbf{W}) \geq 1, \quad \forall k, \\ & \quad \mathbf{W} \succeq \mathbf{0}, \quad \text{Rank}(\mathbf{W}) = 1. \end{aligned} \quad (16)$$

Then SDR drops the rank-one constraint and solves the relaxed SDP. Finally, a rank-one approximate solution of the original problem is retrieved by a Gaussian randomization strategy based on the solution of the relaxed SDP (or simply the principal eigenvector of it). For more details on the SDR algorithms, readers are referred to the key references in the area [39], [40].

### B. Duality between AirComp and Multicast Beamforming

For the special case of a sensor network with single-antenna sensors ( $N_t = 1$ ) and a multi-antenna AP. The receive beamforming reduces to a  $N_r \times 1$  vector denoted by  $\mathbf{f}$ . Its design problem for MMSE AirComp can be directly simplified from problem P5 (which is equivalent to the original P3 when  $N_t = 1$ ) to the following form:

$$\begin{aligned} & \min_{\mathbf{f}} \max_k \|\mathbf{h}_k\|^2 (d_{p_2}^2(\mathbf{u}_k, \mathbf{f}) - 1) \\ & \text{s.t.} \quad \|\mathbf{f}\|^2 = 1, \end{aligned} \quad (17)$$

where  $\mathbf{u}_k$  represents the orientation of the channel vector, i.e.,  $\mathbf{u}_k = \frac{\mathbf{h}_k}{\|\mathbf{h}_k\|}$ .

**Lemma 6.** The solution to the problem (17) is the same as that to the following problem (18) up to a scaling factor.

$$\begin{aligned} & \min_{\mathbf{f}} \|\mathbf{f}\|^2 \\ & \text{s.t.} \quad \|\mathbf{h}_k^H \mathbf{f}\|^2 \geq 1, \quad k = 1, 2, \dots, K. \end{aligned} \quad (18)$$

*Proof:* See Appendix F. ■

**Remark 3** (AirComp-Multicasting Duality). Comparing (15) and (18) reveals that the beamforming problems for the uplink AirComp and downlink multicasting share the same mathematical form. This establishes the AirComp-multicasting duality that is analogous to the famous uplink-downlink duality for multiuser MIMO communication [29]. Intuitively, the AirComp-multicasting duality is a result of the fact that both the AirComp and multicast beamformers must make the same best effort to be aligned with multiple vector channels (see Fig. 3) though for different objectives: one is to minimize the distortion in the computed function value and the other maximize the minimum SNR.

The AirComp beamforming technique designed in the last section is based on computing the weighted centroid on the Grassmann manifold. The duality allows the technique to be applied to multicast beamforming. Compared with the classic

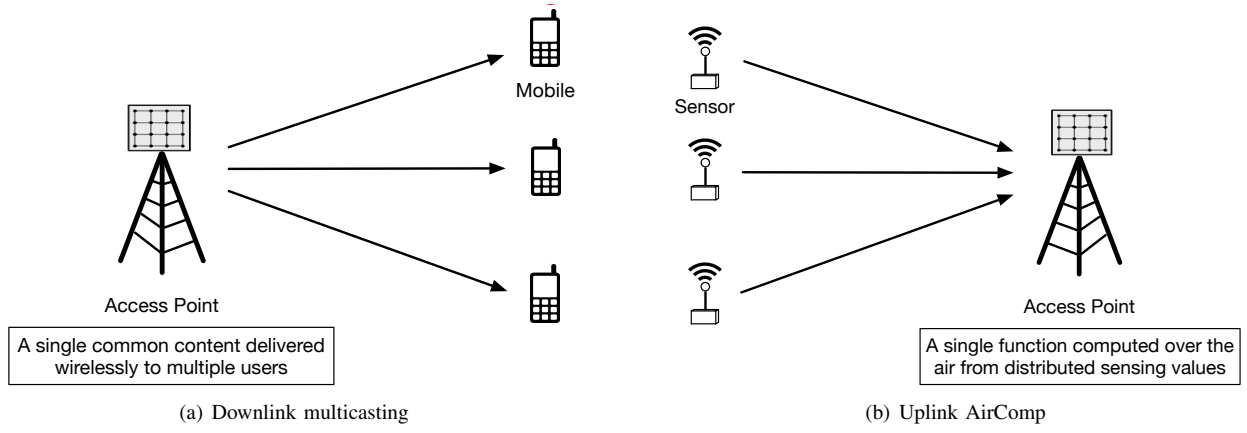


Figure 3. The duality between downlink multicasting and uplink AirComp.

SDR method discussed in the preceding subsection, the AirComp beamforming has the following two main advantages.

- **(Efficient CSI Feedback):** The AirComp beamforming solution requires only the *effective CSI* in (12) and thus enables the efficient “one-shot” channel feedback scheme presented in the next section. In contrast, the SDR solution requires global CSI  $\{\mathbf{h}_k\}$  and thus requires all users to feed back their local CSI. This results in excessive channel training overhead when the number of users is large.
- **(Low Computation Complexity):** As shown in Lemma 5, the weighted centroid solution requires only one-shot computation and has a relatively low complexity of  $O(N_r^2)$  arising from the principal eigenvector calculation. However, the SDR requires first solving a SDP of dimension  $N_r$ , by an iterative interior point method, resulting in the complexity of  $O(\max\{N_r, K\}^4 N_r^{1/2} \log(1/\epsilon))$  where  $\epsilon$  denotes the solution accuracy [40]. The complexity becomes overwhelming when the numbers of the receive antennas and/or users are large. This makes the AirComp solution preferable in practice. The low-complexity advantage of the proposed solution is also verified by simulation in Section VII.

## VI. MULTI-FUNCTION AIRCOMP: CHANNEL FEEDBACK

In this section, the AirComp feedback problem stated in Problem P2 is solved by feedback technique design. Using the optimization results in Section IV, two novel techniques are designed in the following subsections for sequential feedback of two components of the AirComp receive beamformer, namely the normalized beamformer and the denoising factor. Essentially, the two techniques realize the AirComp of two functions: 1) the weighted centroid of a set of matrices and 2) the maximum of a set of scalars, which can be thus implemented using the AirComp architecture in Fig. 2.

### A. Feedback of Normalized Beamformer

Assume that the feedback channel is noiseless due to high transmission power for channel feedback. The AirComp feedback scheme for acquisition of the normalized beamformer  $\mathbf{F}^*$  in (13) is derived as follows. As indicated by Lemma 5, the normalized beamformer  $\mathbf{F}^*$  can be directly computed from

effective CSI matrix  $\mathbf{G}$  in (12). The key step for solving the AirComp feedback problem in Problem P2 is to enforce the equality  $\mathbf{Y} = \mathbf{G}$ . Then given  $\mathbf{G} = \sum_{k=1}^K \lambda_{\min}(\Sigma_k^2) \mathbf{U}_k \mathbf{U}_k^H$  and Let  $\mathbf{H}_k = \mathbf{U}_k \Sigma_k \mathbf{V}_k^H$  denote the compact SVD of  $\mathbf{H}_k$ , it is easy to verify using Problem P2 that designing the feedback signals  $\{\mathbf{X}_k^*\}$  as  $\mathbf{X}_k^* = \lambda_{\min}(\Sigma_k^2) \mathbf{V}_k \Sigma_k^{-1} \mathbf{U}_k^H$  gives the desired equality  $\mathbf{Y} = \mathbf{G}$ . Then the normalized receive beamformer can be computed as the principal eigenvectors of the received signal  $\mathbf{Y} = \mathbf{G}$ . The AirComp feedback design for acquiring  $\mathbf{F}^*$  is summarized as follows.

### Normalized Beamformer Feedback:

- Feedback Signal :  

$$\mathbf{X}_k^* = \tilde{g}_k(\mathbf{H}_k) = \lambda_{\min}(\Sigma_k^2) \mathbf{V}_k \Sigma_k^{-1} \mathbf{U}_k^H,$$
- Received Signal :  

$$\mathbf{Y} = \sum_{k=1}^K \mathbf{H}_k \mathbf{X}_k^*,$$
- Feedback Post Processing :  

$$\mathbf{F}^* = \tilde{f}(\mathbf{Y}) = [\mathbf{U}_Y]_{:,1:L},$$

where  $[\mathbf{U}_Y]_{:,1:L}$  denote the  $L$  dominant left eigenvectors of  $\mathbf{Y}$ . It is important to note that scaling the feedback signal  $\mathbf{X}_k^*$  by a constant so as to meet a transmission power constraint has no effect on the received normalized beamformer  $\mathbf{F}^*$ .

The above AirComp feedback technique inherits the advantage of AirComp by turning interference from multiple access into useful signals for functional computing. In contrast with the traditional method of channel training, increasing the number of simultaneous sensors may even be beneficial to the computation accuracy via sensing-noise averaging.

### B. Feedback of Denoising Factor

Following (14), the denoising factor  $\eta^*$  is the maximum of a set of scalars  $\{\eta_k\}$  called feedback values and defined as:

$$\eta_k = \frac{1}{P_0} \text{tr}(((\mathbf{F}^*)^H \mathbf{H}_k \mathbf{H}_k^H \mathbf{F}^*)^{-1}). \quad (20)$$

Since the maximum is not a nomographic function, it is not directly AirComputable. However, an intelligent feedback technique is presented shortly that shows the possibility of denoising-factor acquisition by AirComp over a fixed number of  $M$  feedback rounds. To begin with, it is assumed that the



normalized beamformer  $\mathbf{F}^*$  is acquired at the AP using the technique in the preceding sub-section and then broadcasts to all sensors. This allows each sensor to apply zero-forcing transmit beamforming for inverting the corresponding channel matrix. Specifically, the transmit beamformer at sensor  $k$  is given as  $\mathbf{B}_k = ((\mathbf{F}^*)^H \mathbf{H}_k)^H ((\mathbf{F}^*)^H \mathbf{H}_k \mathbf{H}_k^H \mathbf{F}^*)^{-1}$ . Such beamforming creates a effective set of *parallel MACs* such that the signal vectors transmitted by sensors are summed at the AP. In other words, with  $\mathbf{e}_k$  denoting the  $N_t \times 1$  signal vector for sensor  $k$ , the receive signal vector at the AP is  $\sum_k \mathbf{e}_k$ . Furthermore, we assume that the denoising factors lie in a fixed finite range  $[\eta_{\min}, \eta_{\max}]$ . Given the parallel MACs and the assumption, the algorithm for denoising-factor feedback with  $M$  feedback rounds is described as follows.

#### Algorithm for Denoising-Factor Feedback:

- 1) **(Initialization):** Set the feedback counter  $n = 1$  and initialize the feedback-quantization range  $[\eta_{\min}^{(n)}, \eta_{\max}^{(n)}]$  with  $\eta_{\max}^{(1)} = \eta_{\max}$ , and  $\eta_{\min}^{(1)} = \eta_{\min}$ .
- 2) **(Feedback Quantization):** A quantizer codebook with  $N_t$  values, denoted by  $\mathbf{Q} = [q_1, q_2, \dots, q_{N_t}]$ , with  $q_1 < q_2 < \dots < q_{N_t}$ , is generated by uniformly partitioning the range  $[\eta_{\min}^{(n)}, \eta_{\max}^{(n)}]$ . Thus, the maximum quantization error  $\epsilon_{\max}$  is bounded by half of each partition interval denoted as  $\Delta$ :  $\epsilon_{\max} \leq \frac{\Delta}{2} = \frac{\eta_{\max}^{(n)} - \eta_{\min}^{(n)}}{2N_t}$ . Quantizing the feedback value  $\eta_k$  in (20) at sensor  $k$  gives the codebook index  $m_k = \arg \min_m |\eta_k - q_m|$ .
- 3) **(Concurrent Feedback):** Each sensor transmits a signal vector comprising a single 1 at the location specified by the corresponding codebook index and 0's at other locations. Specifically, the signal vector  $\mathbf{e}_k$  for sensor  $k$  is

$$\mathbf{e}_k = [0, \dots, 0, 1, 0, \dots, 0], \quad \text{with} \quad [\mathbf{e}_k]_{m_k} = 1. \quad (21)$$

Then all sensors transmit their signal vectors simultaneously over the said effective parallel MACs. The AP finds the largest index of a *nonzero element* in the received signal vector  $\sum_k \mathbf{e}_k$ , denoted as the  $\ell_{\max}$ . Thereby, using the codebook  $\mathbf{Q}$ , it can be inferred at the AP that the quantized value of the denoising factor  $\eta^*$  is  $q_{\ell_{\max}}$  and the exact value lies in the range  $[q_{\ell_{\max}} - \frac{\Delta}{2}, q_{\ell_{\max}} + \frac{\Delta}{2}]$ .

- 4) **(Refining Quantization Range):** To improve the quantization resolution in the next feedback round, the AP refines the quantization range as

$$\eta_{\max}^{(n+1)} = q_{\ell_{\max}} + \frac{\Delta}{2} \quad \text{and} \quad \eta_{\min}^{(n+1)} = q_{\ell_{\max}} - \frac{\Delta}{2}.$$

Next, increase the counter by setting  $n = n + 1$  and go back to 2) if  $n < M$  or otherwise stop the feedback process.

From the above algorithm, the key result on the feedback accuracy follows.

**Proposition 1.** Given  $M$  feedback rounds, the AP receives a quantized version of  $\eta^*$ , denoted as  $\hat{\eta}^*$ , with the quantization error  $\epsilon = |\hat{\eta}^* - \eta^*|$  bounded as

$$\epsilon \leq \frac{\eta_{\max} - \eta_{\min}}{2} N_t^{-M}. \quad (22)$$

Proposition 1 implies that the feedback error reduces exponentially with the number of feedback rounds. Specifically, adding a feedback round improves the feedback resolution by  $\log_2 N_t$  bit. Given a target resolution with the maximum quantization error  $\epsilon_{\max}$ , the required number of feedback rounds by the proposed feedback scheme is given by

$$M = \left\lceil \frac{\log_2(\eta_{\max} - \eta_{\min}) - \log_2 2\epsilon_{\max}}{\log_2 N_t} \right\rceil. \quad (23)$$

As an example, for some practical settings of  $\eta_{\max} = 100$ ,  $\eta_{\min} = 0$ ,  $\epsilon = 10^{-4}$ ,  $N_t = 8$ , the required number of rounds (feedback slots) is  $M = 7$  according to (23). This is much smaller than the number of sensors in a dense network which determines the feedback rounds if the traditional method of channel training is adopted.

**Remark 4** (Comparison with State-of-the-Art). The state-of-the-art algorithm for AirComp of a maximum function was proposed in [3] based on a different principle from the current design. In [3], the maximum of a set of distributed feedback values is progressively computed at the AP by sequential detection of the bits in the binary representation of the desired value via scheduling transmitting sensors by broadcasting a threshold. As the result, each feedback round increases the feedback resolution by a *single bit* and the algorithm cannot be straightforwardly extended to exploit spatial multiplexing. In contrast, by exploiting spatial channels for implementing uniform quantization, the proposed feedback algorithm achieves *multi-bit* resolution improvement for each feedback round as mentioned earlier.

#### C. Comparison with Conventional Channel Training

For conventional multiuser channel training, sensors take turns to transmit pilot signals to AP for uplink channel training to avoid collision (see e.g., [26], [27]). The pilot signal for each sensor should be a  $N_t \times N_t$  or larger matrix for estimating a  $N_r \times N_t$  channel matrix. Thus it takes at least  $T = K \times N_t$  symbol slots to complete the channel training process for a network comprising  $K$  sensors. In contrast, the proposed AirComp feedback technique for normalized beamformer feedback involves simultaneous transmissions of all  $\{\mathbf{X}_k\}$ , each of size  $N_t \times N_r$ , which thus requires only  $N_r$  symbol slots. This together with the  $M$  slots (typically 6–8) for the feedback of the denoising factor yields the total feedback slots of  $N_r + M$  independent of the network size  $K$ . Consider a typical dense sensor network with  $K = 100$ ,  $N_r = N_t = 8$  and  $M = 8$ , it takes only 16 slots for the proposed AirComp feedback scheme in contrast to 800 slots required by the conventional channel training. Thus AirComp feedback achieves 50-time of feedback overhead reduction in this example.

## VII. SIMULATION RESULTS

In this section, the performance of the proposed multi-function AirComp is evaluated by simulation. The simulation parameters are set as follows unless specified otherwise. The number of multi-modal sensors is  $K = 50$ , the AP array size at AP  $N_r = 20$ , the sensor array size and the number of

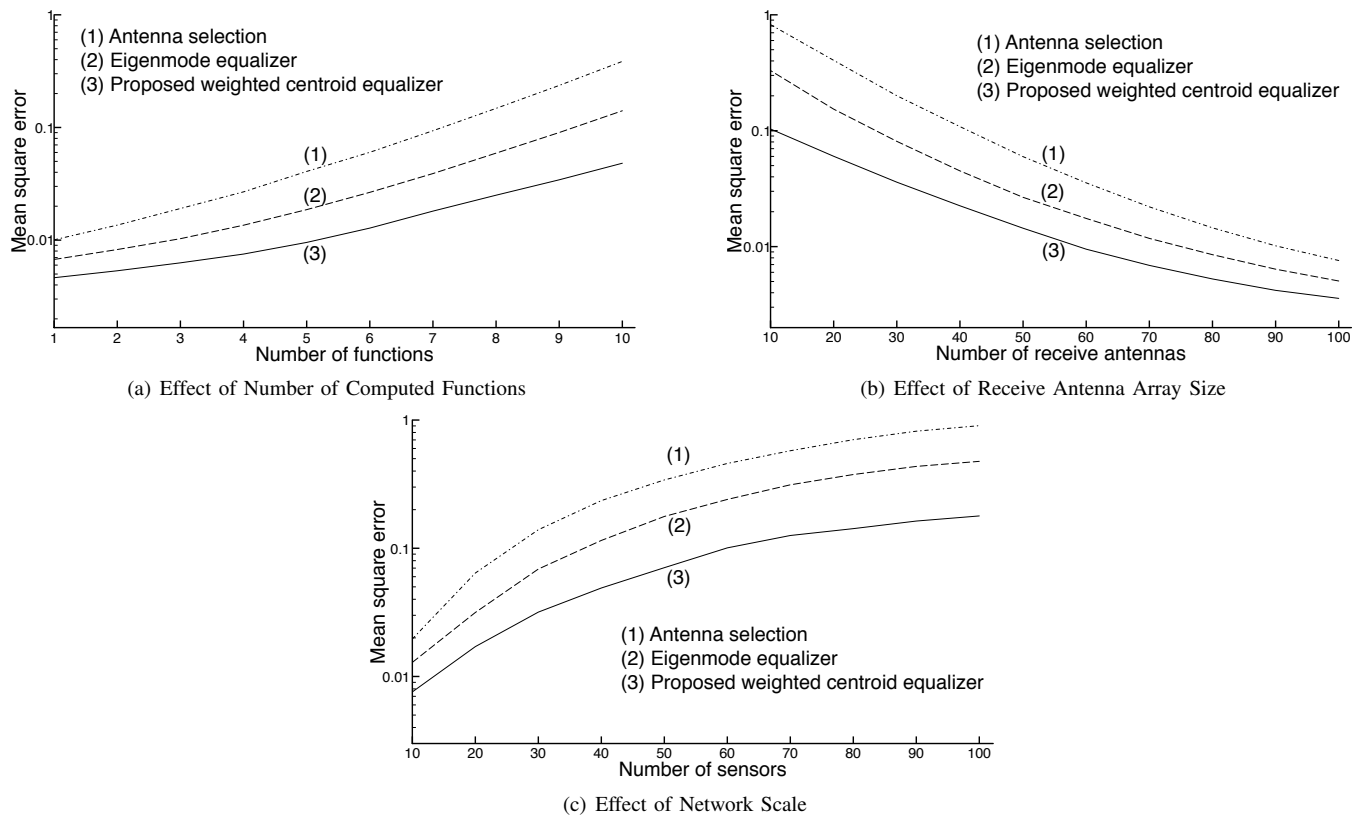


Figure 4. Comparison between the proposed solution and the base line solutions for the case of multiple-function AirComp.

computed functions are equal to  $N_t = L = 10$ . Each MIMO channel are assumed to be i.i.d. *Rician fading*, modelled as i.i.d. complex Gaussian random variables with non-zero mean  $\mu = 1$  and variance  $\sigma_n^2 = 1$ . In addition, the average transmit-SNR constraint, defined as  $\rho_t = P_0/\sigma_n^2$ , is set to be 10 dB.

#### A. Baseline Beamforming Schemes

Given that the optimization of AirComp beamforming is a NP-hard problem, for the purpose of comparison, we consider two baseline AirComp beamforming schemes designed based on the classic approaches, namely *antenna selection* and *eigenmode beamforming*. Both schemes assume zero-forcing transmit beamforming in (7) and their difference lies in the receive beamformers. Define the sum-channel matrix  $\mathbf{H}_{\text{sum}} = \sum_{k=1}^K \mathbf{H}_k$ . To enhance the receive SNRs, the antenna-selection scheme selects the  $L$  receive antennas observing the largest channel gains in the sum channel  $\mathbf{H}_{\text{sum}}$ . Consequently, the effective channel matrix after beamforming consists of  $L$  rows of  $\mathbf{H}_{\text{sum}}$  with largest vector norms. On the other hand, to select the  $L$  strongest eigenmodes of  $\mathbf{H}_{\text{sum}}$  for AirComp, the normalized eigenmode receive beamformer consists of the  $L$  dominant left eigenvectors of  $\mathbf{H}_{\text{sum}}$ . The denoising factor of each type of beamforming design is computed following (14) with  $\mathbf{F}^*$  modified accordingly.

#### B. Performance of Multiple-Function AirComp

In Fig 4, the MSE performance of the proposed multi-function AirComp beamforming is compared with that of two baseline schemes introduced in the preceding subsections. A varying number of functions  $L$ , size of receive array  $N_r$ , and

also number of sensors  $K$  are considered in Fig. 4(a) - 4(c), respectively. Several key observations can be made as follows. First, for all schemes, the MSE is a increasing function of  $L$  and  $K$  but an increasing function of  $N_r$ . This coincides with our intuition that, higher computation throughput is at a cost of declining accuracy, and more connected sensors makes it harder to design one common receive beamformer to equalize all different users' MIMO channels. Nevertheless, deploying more receive antennas compensate for the performance degradation by exploiting diversity gain. Second, under various parameter settings, the proposed scheme outperforms the other two baseline schemes, showing the effectiveness of the new design approach based on optimization on the Grassmann manifold. Furthermore, the performance gain of the proposed design is larger in the regime of large  $L$  and  $K$ , further confirming the effectiveness of the proposed design for multi-modal sensing and dense networks. Last, one can observe that the performance between different schemes converge as  $N_r$  grows. This suggests that the large diversity gain enhances the receive SNRs such that the optimization of AirComp beamforming is less critical and simple designs suffice.

#### C. Comparison with the SDR Method

The discovered AirComp-multicasting duality leads to the availability of two methods, the proposed weighted centroid and the SDR methods, for designing beamforming in either type of systems. Their performance and complexity are compared by simulation as follows. Consider single-antenna uni-modal sensors as in Section V. The comparison of the MSE performance and computation time between the proposed weighted centroid and the SDR solutions is provided

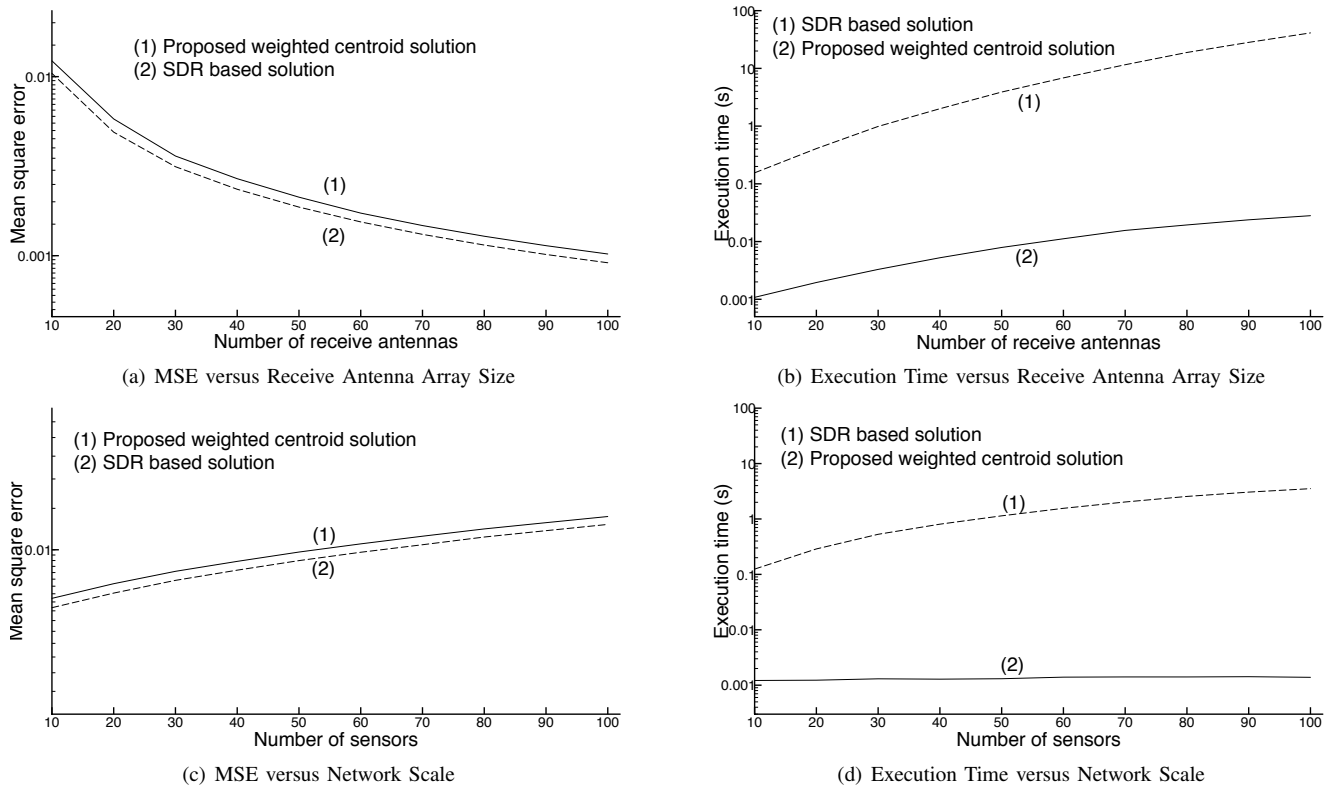


Figure 5. Comparison between the proposed solution and the SDR based solution for the case of single-function AirComp.

in Fig. 5 for the varying receive array size  $N_r$  and number of sensors  $K$ . The computation time is measured using MATLAB. It is observed that the weighted centroid solution can achieve comparable performance as the SDR solution, which is optimal with a high probability for the NP-hard multicast beamforming problem as shown in [40]. On the other hand, the former achieves dramatic computation time reduction with respect to the latter, ranging from 100x to 1000x in the considered ranges of  $N_r$  and  $K$ . The simulation results support our previous analysis in Section V that the complexity of the proposed solution is  $O(N_r^2)$  independent of the network size  $K$  and furthermore insensitive to the variation of the array size  $N_r$ , while the complexity of the SDR solution is  $O(\max\{N_r, K\}^4 N_r^{1/2} \log(1/\epsilon))$ . Thereby, the proposed solution features low complexity and is preferred in the large scale sensor networks (or large scale multicast networks) or when the AP is equipped with a large scale array.

## VIII. CONCLUDING REMARKS

In this paper, we have proposed the framework of multi-function AirComp for MIMO HMM sensor networks. In particular, we have developed an approach for designing receive beamforming using tools from differential geometry. This approach achieves dramatic complexity reduction than the state-of-the-art SDR approach while maintaining comparable performance. Furthermore, building on the AirComp system architecture, intelligent channel feedback techniques have been designed for enabling AirComp beamforming. Unlike the traditional method of channel training, the techniques prevent feedback overhead from escalating with the number of sensors and thus are highly efficient for dense HMM sensor networks. Last, the discovery of AirComp-multicasting duality allows

the low-complexity beamforming design to be transferable to multi-antenna multicast systems, which traditionally relies on the computation-intensive SDR method for beamforming optimization. The work points to the promising new research area of MIMO AirComp where many interesting research issues warrant further investigation such as sensor scheduling, broadband AirComp, AirComp for multi-AP cooperative sensor networks, and AirComp for supporting distributed learning and inference.

## APPENDIX

### A. Preliminaries on Grassmann Manifold

1) *Stiefel and Grassmann Manifolds*: The  $(N, M)$  Stiefel manifold is the set of all  $N$ -by- $M$  tall orthonormal matrices for  $1 \leq M \leq N$ , denoted by  $\mathcal{V}_{N,M}$ . Mathematically,  $\mathcal{V}_{N,M} = \{\mathbf{V} \in \mathbb{C}^{N \times M} : \mathbf{V}^H \mathbf{V} = \mathbf{I}\}$ . On the other hand, the  $(N, M)$  Grassmann manifold is a set of all  $M$ -dimensional subspaces in  $\mathbb{C}^N$ , denoted by  $\mathcal{G}_{N,M}$ . Thereby a Grassmann manifold  $\mathcal{G}_{N,M}$  can be seen as the *quotient space* of  $\mathcal{V}_{N,M}$ . To be specific, a point on the Grassmann manifold corresponds to a class of  $N$ -by- $M$  orthonormal matrices on the Stiefel manifold that span the same column subspace defined by the point. Choosing an arbitrary matrix  $\mathbf{U}$  from this class and using it as a *generator*, the class, denoted as  $[\mathbf{U}]$ , can be mathematically written as  $[\mathbf{U}] = \{\mathbf{U}\mathbf{Q} : \mathbf{Q} \in \mathcal{O}_M\}$  where  $\mathcal{O}_M$  denotes the group of  $M \times M$  unitary matrices. This leads to a relation between the Grassmannian  $\mathcal{G}_{N,M}$  and the Stiefel  $\mathcal{V}_{N,M}$ :  $\mathcal{G}_{N,M} = \mathcal{V}_{N,M}/\mathcal{O}_M$  [38].

2) *Distance Metrics on Grassmann manifold*: Algorithms on Grassmann manifold often involves the calculation of the distance between points on the manifold. There exist many

different distance metrics and all of them are derived from a key notion called *geodesic*. Roughly speaking, a geodesic is the unique curve linking two points on a manifold that has the shortest length among all. The length of the geodesic is called the geodesic distance (or arc length). Mathematically, given  $\mathbf{X}, \mathbf{Y} \in \mathcal{G}_{N,M}$ , their geodesic distance, denoted as  $d^2(\mathbf{X}, \mathbf{Y})$  is calculated by  $d^2(\mathbf{X}, \mathbf{Y}) = \sum_{i=1}^M \theta_i^2$  where  $\{\theta_i\}$  are called the *principal angles*, measuring the minimal angles among any two sets of orthonormal bases spanning the two subspaces [38]. An efficient way to compute the principal angles is to perform SVD on  $\mathbf{X}^H \mathbf{Y}$ , i.e.,

$$\text{(Principal Angles)} \quad \mathbf{X}^H \mathbf{Y} = \mathbf{U} \text{diag}(\cos \theta_i) \mathbf{V}^H, \quad (24)$$

where the singular values in (24) yields the cosines of the principal angles. Based on these angles, a rich set of subspace-distance metrics can be defined. Two particular metrics of relevance in this paper are [38]:

- Projection 2-norm :

$$d_{p_2}(\mathbf{X}, \mathbf{Y}) = \|\mathbf{X}\mathbf{X}^H - \mathbf{Y}\mathbf{Y}^H\|_2 = \|\sin(\boldsymbol{\theta})\|_\infty, \quad (25)$$

- Projection F-norm :

$$d_{p_F}(\mathbf{X}, \mathbf{Y}) = \|\mathbf{X}\mathbf{X}^H - \mathbf{Y}\mathbf{Y}^H\|_F = \|\sin(\boldsymbol{\theta})\|_2, \quad (26)$$

where  $\boldsymbol{\theta}$  is the vector formed by  $\{\theta_i\}_{i=1}^M$ , and matrices  $\mathbf{U}$  and  $\mathbf{V}$  follow those in (24). For  $\mathbf{X} \neq \mathbf{Y}$ , we have the following inequalities relating different distance metrics:

$$d^2(\mathbf{X}, \mathbf{Y}) \geq d_{p_F}(\mathbf{X}, \mathbf{Y}) \geq d_{p_2}(\mathbf{X}, \mathbf{Y}) \geq \frac{1}{\sqrt{M}} d_{p_F}(\mathbf{X}, \mathbf{Y}). \quad (27)$$

### B. Proof of Lemma 1

Given the MSE objective provided in (4), it is easy to note that both the first and the second terms within, i.e.,  $\sum_{k=1}^K ((\mathbf{A}^H \mathbf{H}_k \mathbf{B}_k - \mathbf{I})(\mathbf{A}^H \mathbf{H}_k \mathbf{B}_k - \mathbf{I})^H)$  and  $(\mathbf{A}^H \mathbf{A})$  are positive semidefinite matrix with non-negative eigenvalues. As a result, for any given equalizer  $\mathbf{A}$ , we have the following inequality:

$$\sum_{k=1}^K \text{tr}((\mathbf{A}^H \mathbf{H}_k \mathbf{B}_k - \mathbf{I})(\mathbf{A}^H \mathbf{H}_k \mathbf{B}_k - \mathbf{I})^H) + \sigma_n^2 \text{tr}(\mathbf{A}^H \mathbf{A}) \geq \sigma_n^2 \text{tr}(\mathbf{A}^H \mathbf{A}). \quad (28)$$

It is easy to verify that setting  $\{\mathbf{B}_k\}$  to have the zero-forcing structure in (7) enforces

$$\sum_{k=1}^K \text{tr}((\mathbf{A}^H \mathbf{H}_k \mathbf{B}_k - \mathbf{I})(\mathbf{A}^H \mathbf{H}_k \mathbf{B}_k - \mathbf{I})^H) = 0,$$

and thus achieves the equality in (28), which completes the proof.

### C. Proof of Lemma 2

Utilizing the fact that, for any  $n \times n$  square matrix, the inequality  $\text{tr}(\mathbf{D}^{-1}) \leq n/\lambda_{\min}(\mathbf{D})$  holds, it is straightforward to show

$$\text{tr}((\mathbf{F}^H \mathbf{H}_k \mathbf{H}_k^H \mathbf{F})^{-1}) \leq \frac{L}{\lambda_{\min}(\mathbf{F}^H \mathbf{H}_k \mathbf{H}_k^H \mathbf{F})}. \quad (29)$$

Note that  $\mathbf{F}$  is a tall unitary matrix, thus matrix  $(\mathbf{F}^H \mathbf{H}_k \mathbf{H}_k^H \mathbf{F})$  and  $\mathbf{H}_k \mathbf{H}_k^H$  share the same eigen-spectrum due to the well-known unitary invariant property. Therefore, it is easy to see that the upper bound (29) becomes exact when the channel is well-conditioned.

Then given the compact eigenvalue decomposition  $\mathbf{H}_k \mathbf{H}_k^H = \mathbf{U}_k \Sigma_k^2 \mathbf{U}_k^H$ , we have the following

$$\lambda_{\min}(\mathbf{F}^H \mathbf{H}_k \mathbf{H}_k^H \mathbf{F}) = \lambda_{\min}(\mathbf{F}^H \mathbf{U}_k \Sigma_k^2 \mathbf{U}_k^H \mathbf{F}) \quad (30)$$

$$= \lambda_{\min}(\Sigma_k^2 \mathbf{U}_k^H \mathbf{F} \mathbf{F}^H \mathbf{U}_k) \quad (31)$$

$$\geq \lambda_{\min}(\Sigma_k^2) \lambda_{\min}(\mathbf{U}_k^H \mathbf{F} \mathbf{F}^H \mathbf{U}_k), \quad (32)$$

where the second equality uses the fact that, for arbitrary two matrices  $\mathbf{A}$  and  $\mathbf{B}$  of the same size,  $\mathbf{A}\mathbf{B}$  and  $\mathbf{B}\mathbf{A}$  have the same eigen-spectrum, while the last inequality is due to [41, Corollary 11], and it is easy to verify that the equality holds when  $\Sigma_k^2$  is a scaled identity matrix, namely  $\Sigma_k = \lambda \mathbf{I}$  which also implies the channel is well-conditioned.

Finally, combining (32) and (29) leads to the desired result, which completes the proof.

### D. Proof of Lemma 3

Note that the set of power constraints in P4 can be rewritten as one single constraint by:

$$\eta \geq \max_k \frac{L}{P_0} \frac{1}{\lambda_{\min}(\Sigma_k^2) \lambda_{\min}(\mathbf{U}_k^H \mathbf{F} \mathbf{F}^H \mathbf{U}_k)}. \quad (33)$$

It is easy to note that the minimum  $\eta$  in P4 is achieved when the above constraint is active (the equality holds). Therefore, one can move the constraint in (33) to the objective function and have the following equivalent *min-max* problem:

$$\begin{aligned} \min_{\mathbf{F}} \max_k \frac{L}{P_0} \frac{1}{\lambda_{\min}(\Sigma_k^2) \lambda_{\min}(\mathbf{U}_k^H \mathbf{F} \mathbf{F}^H \mathbf{U}_k)} \\ \text{s.t. } \mathbf{F}^H \mathbf{F} = \mathbf{I}. \end{aligned} \quad (34)$$

The problem in (34) can be further simplified by *max-min* the inverse of the objective function and dropping the constant term  $\frac{L}{P_0}$  which leads to the following form

$$\begin{aligned} \max_{\mathbf{F}} \min_k \lambda_{\min}(\Sigma_k^2) \lambda_{\min}(\mathbf{U}_k^H \mathbf{F} \mathbf{F}^H \mathbf{U}_k) \\ \text{s.t. } \mathbf{F}^H \mathbf{F} = \mathbf{I}. \end{aligned} \quad (35)$$

The objective function in (35) is related to the projection 2-norm Grassmannian metric via

$$d_{p_2}^2(\mathbf{U}_k, \mathbf{F}) = 1 - \lambda_{\min}(\mathbf{U}_k^H \mathbf{F} \mathbf{F}^H \mathbf{U}_k). \quad (36)$$

The equation can be easily verified by using the definitions provided in (24) and (25).

Finally, substituting (36) into (35) leads to the desired problem P5, which completes the proof.

### E. Proof of Lemma 5

In this proof, we first construct an equivalent problem of P7 by modifying the objective function leveraging the orthogonality constraint, giving the problem  $(\mathbf{P}'')$ . Then, we show that solving a relaxed version of  $(\mathbf{P}'')$  without the orthogonality constraint, denoted by  $(\mathbf{P}''')$ , yields a solution enforcing the constraint still. Therefore, one can conclude

that problem P7 and (P''') share the same optimal solution, while the unconstrained problem (P''') can be solved easily by checking all stationary points of the objective. The detailed derivation is presented below.

After some simple algebra manipulation exploiting the linearity of the trace operation, the objective function in (P7) can be further simplified as

$$\sum_{k=1}^K \lambda_{\min}(\Sigma_k^2) \text{tr}(\mathbf{U}_k^H \mathbf{F} \mathbf{F}^H \mathbf{U}_k) = \text{tr}(\mathbf{F}^H \mathbf{G} \mathbf{F}), \quad (37)$$

where  $\mathbf{G}$  is the effective CSI that has been defined in (12). Then problem (P7) reduces to

$$\begin{aligned} (\mathbf{P}') \quad & \max_{\mathbf{F}} \text{tr}(\mathbf{F}^H \mathbf{G} \mathbf{F}) \\ & \text{s.t. } \mathbf{F}^H \mathbf{F} = \mathbf{I}. \end{aligned} \quad (38)$$

Starting with problem (P'), let's first define an alternative objective function  $J(\mathbf{F})$  given by

$$J(\mathbf{F}) = -2\text{tr}(\mathbf{F}^H \mathbf{G} \mathbf{F}) + \text{tr}(\mathbf{F}^H \mathbf{G} \mathbf{F} \mathbf{F}^H \mathbf{F}). \quad (39)$$

It is straightforward to verify that the following problem (P'') is equivalent to problem (P').

$$\begin{aligned} (\mathbf{P}'') \quad & \min_{\mathbf{F}} J(\mathbf{F}) \\ & \text{s.t. } \mathbf{F}^H \mathbf{F} = \mathbf{I}. \end{aligned} \quad (40)$$

Now, let's relax the orthogonality constraint, and consider the following unconstrained problem:

$$(\mathbf{P}''') \quad \min_{\mathbf{F}} J(\mathbf{F}). \quad (41)$$

Since the function  $J(\mathbf{F})$  is a smooth function with gradient defined everywhere, the solution to the problem (P''') should be a stationary point of  $J(\mathbf{F})$ , i.e.,  $\nabla J(\mathbf{F}) = \mathbf{0}$ . It follows that

$$\nabla J(\mathbf{F}) = (-2\mathbf{G} + \mathbf{G} \mathbf{F} \mathbf{F}^H + \mathbf{F} \mathbf{F}^H \mathbf{G}) \mathbf{F} = \mathbf{0}. \quad (42)$$

From (42), one can note that  $\mathbf{F} = \mathbf{0}$  is one of the stationary points.

To seek other stationary points that  $\mathbf{F} \neq \mathbf{0}$ , we left multiply both sides of the equality in (42) with  $\mathbf{F}^H$ , which gives

$$\mathbf{F}^H \nabla J(\mathbf{F}) = \mathbf{F}^H \mathbf{G} \mathbf{F} (\mathbf{F}^H \mathbf{F} - \mathbf{I}) + (\mathbf{F}^H \mathbf{F} - \mathbf{I}) \mathbf{F}^H \mathbf{G} \mathbf{F} = \mathbf{0}. \quad (43)$$

Note that  $\mathbf{F}^H \mathbf{G} \mathbf{F}$  and  $\mathbf{F}^H \mathbf{F} - \mathbf{I}$  are symmetric matrices and  $\mathbf{F}^H \mathbf{G} \mathbf{F}$  is positive definite, thereby one can conclude from (43) that  $\mathbf{F}^H \mathbf{F} = \mathbf{I}$  by invoking the following lemma [42]:

**Lemma 7.** For hermitian matrices  $\mathbf{X}$  and  $\mathbf{Y}$ ,  $\mathbf{X} \mathbf{Y} + \mathbf{Y} \mathbf{X} = \mathbf{0}$  implies  $\mathbf{Y} = \mathbf{0}$  if  $\mathbf{X}$  is positive definite.

Next, substituting  $\mathbf{F}^H \mathbf{F} = \mathbf{I}$  into (42) one can obtain the following equalities that a non-trivial stationary point ( $\mathbf{F} \neq \mathbf{0}$ ) should enforce.

$$\mathbf{G} \mathbf{F} = \mathbf{F} \mathbf{F}^H \mathbf{G} \mathbf{F} \quad \text{and} \quad \mathbf{F}^H \mathbf{F} = \mathbf{I}. \quad (44)$$

It is easy to verify that stationary points satisfying (44) can be represented by  $\mathbf{F} = \mathbf{V}_L \mathbf{Q}$ , where  $\mathbf{V}_L \in \mathbb{C}^{N_r \times L}$  collects  $L$  distinct eigenvectors of  $\mathbf{G}$ , and  $\mathbf{Q}$  is an arbitrary square unitary matrix.

To find the global minimizer of (P'''), we evaluate  $J(\mathbf{F})$  at each stationary point as follows:

- For  $\mathbf{F} = \mathbf{0}$ , we have  $J(\mathbf{F}) = 0$ .
- For  $\mathbf{F} = \mathbf{V}_L \mathbf{Q}$ , we have  $J(\mathbf{F}) = -\text{tr}(\mathbf{Q}^H \mathbf{V}_L^H \mathbf{G} \mathbf{V}_L \mathbf{Q}) = -\text{tr}(\Sigma_L)$ .

where  $\Sigma_L$  is a  $L \times L$  diagonal matrix collecting the eigenvalues corresponding to the eigenvectors selected in  $\mathbf{V}_L$ . Since  $\mathbf{G}$  is positive definite (see (12)), it follows that  $-\text{tr}(\Sigma_L) < 0$ , suggesting  $\mathbf{F} = \mathbf{0}$  is not the global minimizer. Alternatively, one can see that the minimum of  $J(\mathbf{F})$  is achieved by setting  $\mathbf{F}^* = \mathbf{V}_L^* \mathbf{Q}$  with  $\mathbf{V}_L^*$  being the  $L$  principal eigenvectors of  $\mathbf{G}$ . Note that the solution still enforces the orthogonality constraint, and thus also solves problem (P').

#### F. Proof of Lemma 6

Using the definition of the projection 2-norm in (25) together with the fact that  $d_{p_2} = d_{p_F}$  when  $N_t = 1$ , problem in (17) can be rewritten as

$$\begin{aligned} & \max_{\mathbf{f}} \min_k \|\mathbf{h}_k^H \mathbf{f}\|^2 \\ & \text{s.t. } \|\mathbf{f}\|^2 = 1. \end{aligned} \quad (45)$$

Then, by introducing a auxiliary variable  $\rho = \min_k \|\mathbf{h}_k^H \mathbf{f}\|^2$ , the above problem can be equivalently reformulated as follows:

$$\begin{aligned} & \min_{\mathbf{f}, \rho} \frac{1}{\rho} \|\mathbf{f}\|^2 \\ & \text{s.t. } \rho \leq \|\mathbf{h}_k^H \mathbf{f}\|^2, \quad \|\mathbf{f}\|^2 = 1. \end{aligned} \quad (46)$$

Next, changing the optimization variable from  $\mathbf{f}$  to  $\tilde{\mathbf{f}} = \frac{1}{\sqrt{\rho}} \mathbf{f}$ , we can simplify the problem and obtain the desired form in (18). As a result, the solution to (45) can be easily derived by scaling the solution to (18) to meet the unit-norm constraint, which completes the proof.

#### REFERENCES

- [1] M. Agiwal, A. Roy, and N. Saxena, "Next generation 5G wireless networks: A comprehensive survey," *IEEE Commun. Surveys Tuts.*, vol. 18, no. 3, pp. 1617–1655, thirdquarter 2016.
- [2] G. Zhu, S.-W. Ko, and K. Huang, "Inference from randomized transmissions by many backscatter sensors," *IEEE Trans. Wireless Commun.*, vol. PP, no. 99, pp. 1–1, Feb. 2018.
- [3] O. Abari, H. Rahul, and D. Katabi, "Over-the-air function computation in sensor networks," *CoRR*, vol. abs/1612.02307, 2016. [Online]. Available: <http://arxiv.org/abs/1612.02307>
- [4] B. Nazer and M. Gastpar, "Computation over multiple-access channels," *IEEE Trans. Inf. Theory*, vol. 53, no. 10, pp. 3498–3516, 2007.
- [5] S. Zhang, S. C. Liew, and P. P. Lam, "Hot topic: Physical-layer network coding," in *Proceedings of the 12th annual international conference on Mobile computing and networking*. Los Angeles, California, USA.: ACM, Sep. 2006, pp. 358–365.
- [6] M. Gastpar, "Uncoded transmission is exactly optimal for a simple Gaussian sensor network," *IEEE Trans. Inf. Theory*, vol. 54, no. 11, pp. 5247–5251, Nov 2008.
- [7] R. Soundararajan and S. Vishwanath, "Communicating linear functions of correlated Gaussian sources over a MAC," *IEEE Trans. Inf. Theory*, vol. 58, no. 3, pp. 1853–1860, March 2012.
- [8] J. J. Xiao, S. Cui, Z. Q. Luo, and A. J. Goldsmith, "Linear coherent decentralized estimation," *IEEE Trans. Signal Process.*, vol. 56, no. 2, pp. 757–770, Feb 2008.
- [9] C. H. Wang, A. S. Leong, and S. Dey, "Distortion outage minimization and diversity order analysis for coherent multiaccess," *IEEE Trans. Signal Process.*, vol. 59, no. 12, pp. 6144–6159, Dec 2011.
- [10] M. Goldenbaum, S. Stańczak, and H. Boche, "On achievable rates for analog computing real-valued functions over the wireless channel," in *2015 IEEE International Conference on Communications (ICC)*, June 2015, pp. 4036–4041.

- [11] M. Goldenbaum and S. Stanczak, "On the channel estimation effort for analog computation over wireless multiple-access channels," *IEEE Wireless Commun. Lett.*, vol. 3, no. 3, pp. 261–264, June 2014.
- [12] —, "Robust analog function computation via wireless multiple-access channels," *IEEE Trans. Commun.*, vol. 61, no. 9, pp. 3863–3877, September 2013.
- [13] M. Goldenbaum, H. Boche, and S. Stańczak, "Harnessing interference for analog function computation in wireless sensor networks," *IEEE Trans. Signal Process.*, vol. 61, no. 20, pp. 4893–4906, Oct 2013.
- [14] O. Abari, H. Rahul, D. Katabi, and M. Pant, "Airshare: Distributed coherent transmission made seamless," in *Proc. IEEE Conference on Computer Communications (INFOCOM)*, Apr. 2015, pp. 1742–1750.
- [15] S. Sigg, P. Jakimovski, and M. Beigl, "Calculation of functions on the RF-channel for IoT," in *Proc. IEEE International Conference on the Internet of Things*, Oct. 2012, pp. 107–113.
- [16] A. Kortke, M. Goldenbaum, and S. Stańczak, "Analog computation over the wireless channel: A proof of concept," in *Proc. IEEE SENSORS*, Nov. 2014, pp. 1224–1227.
- [17] B. Nazer and M. Gastpar, "Compute-and-forward: Harnessing interference through structured codes," *IEEE Trans. Inf. Theory*, vol. 57, no. 10, pp. 6463–6486, Oct. 2011.
- [18] T. Yang and I. B. Collings, "On the optimal design and performance of linear physical-layer network coding for fading two-way relay channels," *IEEE Trans. Wireless Commun.*, vol. 13, no. 2, pp. 956–967, Feb. 2014.
- [19] L. Shi, S. C. Liew, and L. Lu, "On the subtleties of  $q$ -pam linear physical-layer network coding," *IEEE Trans. Inf. Theory*, vol. 62, no. 5, pp. 2520–2544, May 2016.
- [20] J. Zhan, B. Nazer, U. Erez, and M. Gastpar, "Integer-forcing linear receivers," *IEEE Trans. Inf. Theory*, vol. 60, no. 12, pp. 7661–7685, Dec. 2014.
- [21] A. Sakzad, J. Harshan, and E. Viterbo, "Integer-forcing MIMO linear receivers based on lattice reduction," *IEEE Trans. Wireless Commun.*, vol. 12, no. 10, pp. 4905–4915, Oct. 2013.
- [22] B. Nazer and M. Gastpar, "Reliable physical layer network coding," *Proceedings of the IEEE*, vol. 99, no. 3, pp. 438–460, Mar. 2011.
- [23] J. Gubbi, R. Buyya, S. Marusic, and M. Palaniswami, "Internet of things (IoT): A vision, architectural elements, and future directions," *Future generation computer systems*, vol. 29, no. 7, pp. 1645–1660, Sep. 2013.
- [24] R. K. Ganti, F. Ye, and H. Lei, "Mobile crowdsensing: current state and future challenges," *IEEE Commun. Mag.*, vol. 49, no. 11, pp. 32–39, Nov. 2011.
- [25] G. J. Foschini, "Layered space-time architecture for wireless communication in a fading environment when using multi-element antennas," *Bell Labs Technical Journal*, vol. 1, no. 2, pp. 41–59, 1996.
- [26] D. Gesbert, M. Kountouris, R. W. Heath Jr, C.-B. Chae, and T. Salzer, "Shifting the MIMO paradigm," *IEEE Signal Process. Mag.*, vol. 24, no. 5, pp. 36–46, Sep. 2007.
- [27] Q. H. Spencer, C. B. Peel, A. L. Swindlehurst, and M. Haardt, "An introduction to the multi-user MIMO downlink," *IEEE Commun. Mag.*, vol. 42, no. 10, pp. 60–67, Oct. 2004.
- [28] G. Zhu, K. Huang, V. K. Lau, B. Xia, X. Li, and S. Zhang, "Hybrid beamforming via the Kronecker decomposition for the millimeter-wave massive MIMO systems," *IEEE J. Sel. Areas Commun.*, vol. 35, no. 9, pp. 2097–2114, Jun. 2017.
- [29] N. Jindal, S. Vishwanath, and A. Goldsmith, "On the duality of Gaussian multiple-access and broadcast channels," *IEEE Trans. Inf. Theory*, vol. 50, no. 5, pp. 768–783, May 2004.
- [30] W. Yu, "Uplink-downlink duality via minimax duality," *IEEE Trans. Inf. Theory*, vol. 52, no. 2, pp. 361–374, Feb. 2006.
- [31] E. Bjornson, M. Bengtsson, and B. Ottersten, "Optimal multiuser transmit beamforming: A difficult problem with a simple solution structure [lecture notes]," *IEEE Signal Process. Mag.*, vol. 31, no. 4, pp. 142–148, Jul. 2014.
- [32] D. J. Love and R. W. Heath, "Limited feedback unitary precoding for spatial multiplexing systems," *IEEE Trans. Inf. Theory*, vol. 51, no. 8, pp. 2967–2976, Aug. 2005.
- [33] J. Choi, B. Mondal, and R. W. Heath, "Interpolation based unitary precoding for spatial multiplexing MIMO-OFDM with limited feedback," *IEEE Trans. Signal Process.*, vol. 54, no. 12, pp. 4730–4740, Dec. 2006.
- [34] S. W. Peters and R. W. Heath, "Cooperative algorithms for MIMO interference channels," *IEEE Transactions on Vehicular Technology*, vol. 60, no. 1, pp. 206–218, Jan. 2011.
- [35] A. Medra and T. N. Davidson, "Incremental grassmannian feedback schemes for multi-user MIMO systems," *IEEE Trans. Signal Process.*, vol. 63, no. 5, pp. 1130–1143, Mar. 2015.
- [36] D. J. Love, R. W. Heath, V. K. Lau, D. Gesbert, B. D. Rao, and M. Andrews, "An overview of limited feedback in wireless communication systems," *IEEE J. Sel. Areas Commun.*, vol. 26, no. 8, 2008.
- [37] K. Huang and V. K. Lau, "Stability and delay of zero-forcing SDMA with limited feedback," *IEEE Trans. Inf. Theory*, vol. 58, no. 10, pp. 6499–6514, Oct. 2012.
- [38] A. Edelman, T. A. Arias, and S. T. Smith, "The geometry of algorithms with orthogonality constraints," *SIAM journal on Matrix Analysis and Applications*, vol. 20, no. 2, pp. 303–353, Oct. 1998.
- [39] N. D. Sidiropoulos, T. N. Davidson, and Z.-Q. Luo, "Transmit beamforming for physical-layer multicasting," *IEEE Trans. Signal Process.*, vol. 54, no. 6, pp. 2239–2251, 2006.
- [40] Z.-Q. Luo, W.-K. Ma, A. M.-C. So, Y. Ye, and S. Zhang, "Semidefinite relaxation of quadratic optimization problems," *IEEE Signal Process. Mag.*, vol. 27, no. 3, pp. 20–34, May 2010.
- [41] F. Zhang and Q. Zhang, "Eigenvalue inequalities for matrix product," *IEEE Trans. Auto. Control*, vol. 51, no. 9, pp. 1506–1509, Sep. 2006.
- [42] H. Lütkepohl, "Handbook of matrices." *John Wiley & Sons*, 1997.